Current Research in Toxicology 2 (2021) 19–29

Contents lists available at ScienceDirect

Current Research in Toxicology

journal homepage: www.elsevier.com/locate/crtox

In vitro assays for characterization of distinct multiple catalytic activities of thyroid peroxidase using LC-MS/MS

Abhishek Tater, Aditi Gupta, Gopal Upadhyay, Abhay Deshpande, Rahul Date *, Irfan Y. Tamboli *

Jai Research Foundation, N. H. 48, Near Daman-Ganga bridge, Valvada 396105, India

ARTICLE INFO

ABSTRACT

A diverse set of environmental contaminants have raised a concern about their potential adverse effects on endocrine signaling. Robust and widely accepted battery of *in vitro* assays is available to assess the disruption of androgenic and estrogenic pathways. However, such definitive systems to investigate effects on the disruption of thyroid pathways by the xenobiotics are not yet well established. One of the major "Molecular Initiating Events" (MIEs) in thyroid disruption involves targeting of thyroid peroxidase (TPO), a key enzyme involved in thyroid hormone synthesis. TPO catalyzes mono- and diiodination of L-Tyrosine (L-Tyr) to generate 3-Iodo-L-tyrosine (MIT) and 3,5-Diiodo-L-tyrosine (DIT), respectively, followed by the coupling of iodinated tyrosine rings to generate thyroid hormones, 3,3'5-Triiodo-L-thyronine (T3) and Levothyroxine (T4).

We sought to develop a robust, sensitive, and rapid *in vitro* assay systems to evaluate the effects of test chemicals on the multiple catalytic activities of thyroid peroxidase. Simple *in vitro* assays were designed to study TPO mediated distinct reactions using a single LC-MS/MS method.

Herein, we describe a battery of assays to investigate the iodination of L-Tyr to MIT and DIT, MIT to DIT as well as, T3 to T4 catalyzed by rat thyroid TPO. Importantly, two sequential reactions involving mono- and diiodination of L-Tyr could be analyzed in a single assay. The assay that monitors *in vitro* conversion of DIT to T4 was developed to study the coupling of tyrosine rings. Enzyme kinetics studies revealed distinct characteristics of multiple reactions catalyzed by TPO. Further, the known TPO inhibitors were used to assess their potency towards individual TPO substrates and reactions. The resultant half maximum inhibitory concentration (IC_{50}) values highlighted differential targeting of TPO catalyzed reactions by the same inhibitor. Overall results underscore the need to develop more nuanced approaches that account for distinct multiple catalytic activities of TPO.

1. Introduction

The endocrine system comprises a multitude of hormones, their cellular receptors, and a complex network of glands that co-ordinate internal physiology as well as adaptation to environmental changes. A wide variety of xenobiotics can act as endocrine disruptors (EDs) by perturbing naturally occurring hormones. This in turn could alter synthesis, release, action, or elimination of the natural hormones. As a cascading effect, such xenobiotics could adversely impact development, reproduction, neurological function, and immune responses. During the 1990s, heightened concerns about the effects of endocrine disruptors on human health and wildlife prompted the development of multiple screening and testing strategies, which are continuously being updated. Several testing strategies and assays have been adopted into guidelines by regulatory agencies such as the organization for economic co-operation and development (OECD) (OECD GD 150, 2018), the office of prevention, pesticides, and toxic substances (OPPTS) (EPA – Series 890, 2009), and others. Early efforts to develop methods to identify estrogen and androgen signaling disruption were later extended to the assessment of steroidogenesis and thyroid signaling.

Disruptions of thyroid hormone (TH) signaling adversely impacts the function of several target tissues in humans and wildlife (Portman, 2008; Younggren & Hadley, 1981). The hypothalamus-pituitary thyroid (HPT) axis regulates TH synthesis via thyroid-stimulating hormone (TSH), secreted from the pituitary. TSH stimulates the synthesis and release of thyroid hormones (THs) by thyroid glands. Sodium/iodide symporter (NIS) mediated uptake of iodide ions by the thyroid is necessary to synthesize THs (Chung, 2002; Tazebay et al., 2000). Oxidation of iodide ions is catalyzed by the multi-substrate specific heme-containing enzyme, TPO (Mclachlan and Rapoport, 1992). The reaction of TPO with the first substrate, hydrogen peroxide (H_2O_2), generates an oxidized enzyme, which oxi-

* Corresponding authors.
E-mail addresses: Rahul.date@jrfonline.com (R. Date), Iytamboli@gmail.com (I.Y. Tamboli).

https://doi.org/10.1016/j.crtox.2021.01.001
Received 11 September 2020; Revised 30 December 2020; Accepted 5 January 2021

dizes the second substrate iodide to generate highly reactive iodine (Davidson et al., 1978b). Subsequent covalent linking of iodine with thyroglobulin tyrosyl residues generates MIT and DIT. While the process of formation of T4 is MIT to DIT, and Two DITs making up T4, there is always a small amount of Triiodothyronine, or T3, formed when an MIT binds with DIT. The proteolysis of thyroglobulin stimulated by TSH in thyroid follicular epithelial cells releases T4 and T3 in circulation. Even though only about 20% of T3 originates from the thyroid gland, 80% comes from peripheral conversion via a deiodinase. (Pirahanchi et al., 2020).

EDs can perturb the HPT regulatory axis at multiple levels by affecting, NIS and TPO activity. This includes release, transport, and extrathyroidal uptake of THs; binding of TH to nuclear receptors, and clearance of THs by liver. TH metabolism also involves deiodination to convert inactive prohormone, T4 to the active form, T3. The HPT regulatory axis regulates gene expression of proteins involved in the above processes. (Bianco & Kim, 2006). Due to its vulnerability to several known natural and man-made chemicals, inhibition of TPO catalytic activity has been widely accepted as an MIE in the TH signaling disruption (Coady et al., 2010; Davidson et al., 1978a; Hornung et al., 2010; Serrano et al., 2010; Tietge et al., 2005, 2010).

Diverse compounds including natural dietary polyphenols from parsley, green tea/coffee, cumin, mustard, amino acids as well as synthetic environmental xenobiotic such as pesticides are known to inhibit TPO (Doerge & Chang, 2002; Ferreira et al., 2000; Lerro et al., 2018). The Daily consumption/exposure and bioavailability in the target tissue (thyroid) are perhaps the key factors for the cause of potential adverse effects leading to disruption in TH signaling (Fini et al., 2017). Anti-hyperthyroidism medications methimazole (MMI) and 6-propyl-2-thiouracil (PTU) are known to disrupt TH synthesis in humans and many other animal species (Boas et al., 2012; Davidson et al., 1978a; Gilbert et al., 2012; Haselman et al., 2020; Motonaga et al., 2016). MMI and PTU are often used as positive controls in *in vivo* and *in vitro* studies. Additionally, HTS assays have identified several hundreds of the TPO inhibitors such as Quercetin, Apigenin, Genistein and Daidzein which belongs to the natural polyphenols (Paul Friedman et al., 2016). Decomposition product of widely used ethylene bis dithiocarbamate (EBDC), Ethylenethiourea (ETU), is one of the major xenobiotics which can adversely impact TPO activity. Importantly, the exposure to TPO inhibitors during early gestation could potentially affect the development and even moderate reduction in TH levels during early stages can cause irreversible neurological damages leading to cognitive and learning deficits. This accentuates the need to identify the chemicals that interfere with TH homeostasis by inhibiting TPO or any other relevant mechanisms.

Multiple assays that analyze the oxidation of indicator dyes facilitated by TPO in the presence of H_2O_2 and iodide have been reported before. The most used *in vitro* assay relies upon TPO catalyzed, H_2O_2 dependent oxidation of guaiacol to yellowish-brown diguaiacol which can be detected spectrophotometrically (Chang & Doerge, 2000; HOSOYA & MORRISON, 1965). A commercially available fluorogenic substrate, Amplex UltraRed (AUR) with horse-radish peroxidase was also successfully repurposed to detect TPO activity for high-throughput screening (HTS) of xenobiotics (Paul et al., 2014). Additionally, TPO mediated oxidation of luminol and subsequent measurement of luminescence has also been used to evaluate TPO activity (Kaczur et al., 1997). Some of these assays were employed by ToxCast and Tox21 programs for HTS of TPO inhibitors (Celi et al., 2008; Paul Friedman et al., 2016; Martin et al., 2007, 2009; Orloff et al., 2018).

Assays that make use of indicator dyes provide information about iodine oxidation by TPO. However, as described above, TPO catalysis is characterized by multiple distinct reactions that encompass oxidation of iodine, multiple substrate iodination reactions, and coupling of tyrosine phenolic rings to generate T3 and T4. Iodination and phenolic coupling, two-electron transfer v/s one-electron transfer, respectively, are two distinct reactions catalyzed by TPO (Nakamura et al., 1984). Although iodination is believed to be a non-specific reaction, substrate-specific differences have been reported (Kootstra et al., 1993). It is also possible that thyroid disruptors could target different reactions catalyzed by TPO, at the specific steps. However, currently published assays do not discriminate between their mode of action, neither do these assays enable effective monitoring and investigation of individual reactions.

Here, we describe a unique strategy, based on a battery of *in vitro* assays, and a highly sensitive, specific multiple reaction monitoring (MRM) using LC-MS/MS, to comprehensively analyze the multiple catalytic activities of TPO and characterize each of the distinct reaction catalyzed by this enzyme. Rat thyroid microsomes were used as TPO source. Successful conversion of L-Tyr to MIT and DIT, MIT to DIT, DIT to T4, and, T3 to T4 can be studied effectively by these assays. The approach suggested here, enables substrate and end product-specific reaction analysis of iodine organification into L-Tyr as well as allow investigation of coupling of iodized tyrosyl rings to generate THs. Such enhanced mechanistic understandings into TPO catalysis will facilitate the discrimination between diverse TPO inhibitors. Overall, the proposed strategy can be used as an important tool to further elucidate the TPO catalysis, address the impact of thyroid disruptors on TPO activity, and enable their pertinent categorization.

2. Materials and methods

2.1. Reagent and chemicals

L-Tyrosine disodium salt hydrate (CAS 69847-45-6) was obtained from the Tokyo chemical industry, Japan. L- Tyrosine (CAS 60-18-4, Reagent grade), 3-Iodo-L-tyrosine (MIT, CAS 70-78-0), 3,5-Diiodo-L-tyrosine dehydrate (DIT, CAS 18835-59-1), 3,3′,5- Triiodo-L-thyronine (Levothyronine, T3, CAS 6893-02-3), 3,3′,5,5′-Tetraiodo-L-thyronine (Levothyroxine, T4, CAS 51-48-9), Apigenin (AGN, CAS 520–36-5), Daidzein (DZN, CAS 486-66-8), Ethylenethiourea (2-Imidazolidinethione, ETU, CAS 96–45-7), Genistein (GST, CAS 446-72-0), 6-Propyl-2-thiouracil, PTU, CAS 51-52-5), Testosterone (TST, CAS 58–22-0), Dimethyl sulfoxide (DMSO, CAS 67-68-5, Laboratory Reagent grade), Oxalic acid (CAS 144–62-7, Analytical Reagent grade), Protease Inhibitor cocktail (Product code P8340), Cell dissociation sieve - tissue grinder kit (Product code CD1), Potter Elvehjem polytetrafluoroethylene (PTFE) assembly, Sodium thiosulfate (CAS 7772-98-7) and Ethylenediaminetetraacetic acid (EDTA, CAS 6381-92-6, Molecular Biology grade) were procured from Sigma-Aldrich, India. Potassium Iodide (KI, CAS 7681-11-0, Excellent Analytical Reagent grade) and Hydrogen peroxide solution (H_2O_2, 30% w/w, CAS 7722-84-1, Super Quality grade) were obtained from Qualigens, India. Glycerol (Glycerin) Anhydrous (CAS 56-81-5, Analytical Reagent grade) was got from Srlchem. Dulbecco's phosphate buffered Saline (DPBS, 1X, Ref 14191-144) was received from Gibco. Sucrose (Ref RM 3063, Analytical Reagent grade) was purchased from HIMEDIA. Acetonitrile (CAS 75-05-8, ULC/MS grade) was taken from Biosolve. Formic acid (98–102%, CAS 64-18-6, HPLC grade) was supplied by Merck. Water (Milli-Q, Type-2) was taken from Milli-Q Advantage A10 Merck Laboratory water purification system. Bicinchoninic acid (BCA) kit for protein estimation was procured from Pierce.

2.2. Microsome isolation

The usage of rats for thyroid isolation was taken after obtaining approval from the Institutional Animal Ethics Committee. Twelve weeks old male Wistar rats were perfused with 0.9% saline before the thyroid isolation. The collected thyroids were stored at −80 °C. Thyroids from 20 rats were pooled together for microsome isolation (Abas & Luschnig, 2010). Pooled thyroid glands were thawed on ice

and cut into fine pieces using a sterile surgical blade in a DPBS -EDTA containing a protease inhibitor cocktail, followed by homogenization using Potter Elvehjem PTFE assembly. Approximately, 3 mL of DPBS-EDTA was used for the homogenization of thyroid from 20 animals. Cell dissociation sieve - tissue grinder kit was used to further separate and grind bigger pieces left behind. The homogenized tissue suspension was then passed through a 23G needle 15–20 times. An equal volume of 50% sucrose was added to the homogenized tissue suspension and the tubes were centrifuged at 600 × *g* for 5 min at 4 °C. The pellet was discarded, and the supernatant was collected in fresh tubes, and an equal volume of sterile water was added to them. Homogenized tissue suspension, 250 μL, was distributed equally in multiple tubes and centrifuged at 20,000 × *g* for 2 h at 4 °C. The supernatant was discarded. The microsome pellet was pooled and resuspended in 1 mL 5% glycerol-DPBS. Aliquots of microsomes were stored at −80 °C till further use. The protein content of the microsome was estimated using the BCA kit.

2.3. TPO activity assay

The assay was conducted in 250 μL DPBS using thyroid microsomes. KI, H_2O_2, and the microsome protein concentrations were optimized for each batch of the microsomes. KI was used at 150 μM concentration for the initial experiments. We noted a dose-dependent increase in TPO activity when KI concentration was increased to 300 μM. KI concentration was hence kept constant at 300 μM for all the following experiments. The range of concentrations for each substrates L-Tyr, MIT, DIT, and T3 used for optimization experiments is reported in the results section. Upon optimization, L-Tyr was used at 50–100 μM, whereas MIT, DIT, T3 were used at 600 μM. The assay mixture was pre-incubated for a minimum of 10 min, with microsomes and the other reagents, except H_2O_2. The optimum range of H_2O_2 and protein concentration was 40–80 μM and 5–10 μg (for 250 μL assay volume), respectively. 25 μL reaction mixture was aliquoted at desired time points 10, 30 and 60 min, followed quenching with 50 μL ice-cold oxalic acid (750 mM), and 1000 μL acetonitrile containing Rolipram as an internal standard (IS). The tubes were vortexed and centrifuged at 8000 rpm for 5 min at 5 °C. The supernatant was transferred to fresh 1 mL auto-sampler glass shell vials. Samples were loaded into an auto-sampler tray, and 10 μL was injected into LC-MS/MS. Control assays, in the absence of microsomes, H_2O_2, KI, the respective substrate (L-Tyr or MIT or DIT or T3) were set up under similar conditions. The reaction volumes were adjusted with DPBS.

2.4. Concentration-response assays, IC50 analysis

Individual IC_{50} reaction assays contained either L-Tyr at 50 μM, or MIT/DIT/T3 at 600 μM concentrations, with respective test compound at the appropriate concentration, and KI, thyroid microsomes as well as H_2O_2. In the initial experiments, ten concentrations of AGN, DZN, GST, PTU, and TST ranging from 0.015 μM to 330 μM and nine concentrations of ETU ranging from 0.007 μM to 100 μM were used to evaluate their potency to inhibit the conversion of L-Tyr to MIT, L-Tyr to DIT, MIT to DIT and T3 to T4. However, due to precipitation of at higher concentrations of test compounds in the presence of DIT, seven concentrations of GST and PTU ranging from 0.015 μM to 11.859 μM, ten concentrations of DZN, and TST ranging from 0.015 μM to 330 μM, nine concentrations of ETU ranging from 0.007 μM to 100 μM were used, as described in results. Other than ETU, which was dissolved in water, other test compound stocks were made in DMSO. IC_{50} assay was also set up with corresponding DMSO concentration, ranging from 0.0001 to 3% (v/v). The results established that DMSO concentrations used did not affect TPO activity (data not included). Reactions were stopped with oxalic acid-acetonitrile as described above. The prepared sample vials were loaded into an auto-sampler tray, and 10 μL volume was injected to LC-MS/MS sequentially.

2.5. LC-MS/MS conditions

Chromatographic separation of analytes was obtained using HPLC (Exion-LC Sciex) equipped with X-bridge-C18 column of 3.5 μm particle size, 3.0 × 150 mm (i.d. × L) specification. The oven temperature was maintained at 40 °C. The total run time per sample was 4 min at a constant flow rate of 0.550 mL/min. Mobile phase gradient consisted of A: Acetonitrile B: 0.1% formic acid (v/v) from 85% B, till 0.1 min, next gradient was adjusted to 5% B, till 1 min, maintained at same till 3 min, it was returned to 85% B till 4 min. The retention time for MIT, DIT, and T4 mass transitions was 1.43, 1.96, and 2.17 min, respectively.

Linear ion trap quadrupole, QTRAP 5500 LC-MS/MS (AB Sciex) was used for mass spectrometric analysis. Electrospray ionization (ESI) of analytes was followed by detection in positive polarity using MRM (Guo et al., 2012). The ion source was maintained at 550 °C, ion spray voltage at 5500 V, GS1, and GS2 at 65 and 55 psi, respectively. Curtain gas was used at 35 psi, and CAD gas was set to medium. Entrance potential (EP) and collision exit potential (CXP) were 10 and 15 V, respectively. MRM transitions and other parameters are described in Table 1.

2.6. Data analysis and statistics

Analyst 1.7.1 software was used to acquire the data in AB Sciex QTRAP 5500 LC-MS/MS instrument. The Peak area of the metabolite was quantified using the analyst classic integration algorithm. Peak area and area ratio were calculated by Analyst software. Bar and scatter graphs were generated using Microsoft excel 2016. IC_{50}, V_{max} and K_m values were calculated by employing GraphPad Prism. One-way ANOVA analysis using Dunnett's multiple comparisons test was performed for a representative 30 min incubation period compared with control with Prism. Each experiment was repeated three times, and data from a representative experiment is shown in the manuscript. Data from multiple experiments with IC50 values and standard deviations (SD) are shown in Fig. 5.

3. Results

3.1. Method development for the analysis of THs and their synthesis intermediates using LC-MS/MS

LC-MS/MS based MRM approach was developed to monitor the multiple reactions catalyzed by TPO. Highly selective and sensitive MRM scan methods were established to analyze mass transitions of parent and daughter fragment ions of MIT, DIT, and T4. Q1 and Q3 mass-transitions and their respective collision energies for individual metabolites are shown in Table 1. Representative MS/MS spectra for MIT (Fig. 1A, B), DIT (Fig. 1C), and T4 (Fig. 1D) show the presence of predominant fragment species. Peak area ratio of MIT, DIT and T4 formation was correlated with known concentrations of calibration standards. For the preparation of the calibration curve, rat heat-inactivated thyroid microsomes were used to match the matrix (Supplementary Fig. 1A–C). The correlation coefficients (r) were 0.9967, 0.9949 and 0.9942 for 0.547, 0.273 and 1.094 nM lower (LLOQ) to 270 nM upper limit of quantification (ULOQ) concentration for MIT, DIT and T4 respectively, using linear regression equation with least squared weighting factor (1/x) (Supplementary Fig. 1D). The calibration curves using standards of MIT, DIT and T4 were shown in Supplementary Fig. 1A–C. The other chromatographic and mass spectrometry parameters are described under the methods sections.

Table 1
MRM parameters and mass transitions of MIT, DIT, T4, and rolipram: Compound dependent parameters of MRM transitions for MIT, DIT, T4, and rolipram were optimized and respective dwell time (ms), declustering potential (DP), and collision energy (CE) are shown here. Monitored parents and fragment ions (*m/z*, Q1/Q3) are listed in the table.

Compound	Q1 (*m/z*)	Q3 (*m/z*)	Dwell Time (ms)	DP (V)	CE (eV)
3- Monoiodotyrosine (MIT)	308	262/135	150	55	25/40
3,5- Diiodotyrosine (DIT)	434	388	100	65	25
Levothyroxine (T4)	778	732	110	50	30
Rolipram (Internal standard)	276	208.3	95	80	23

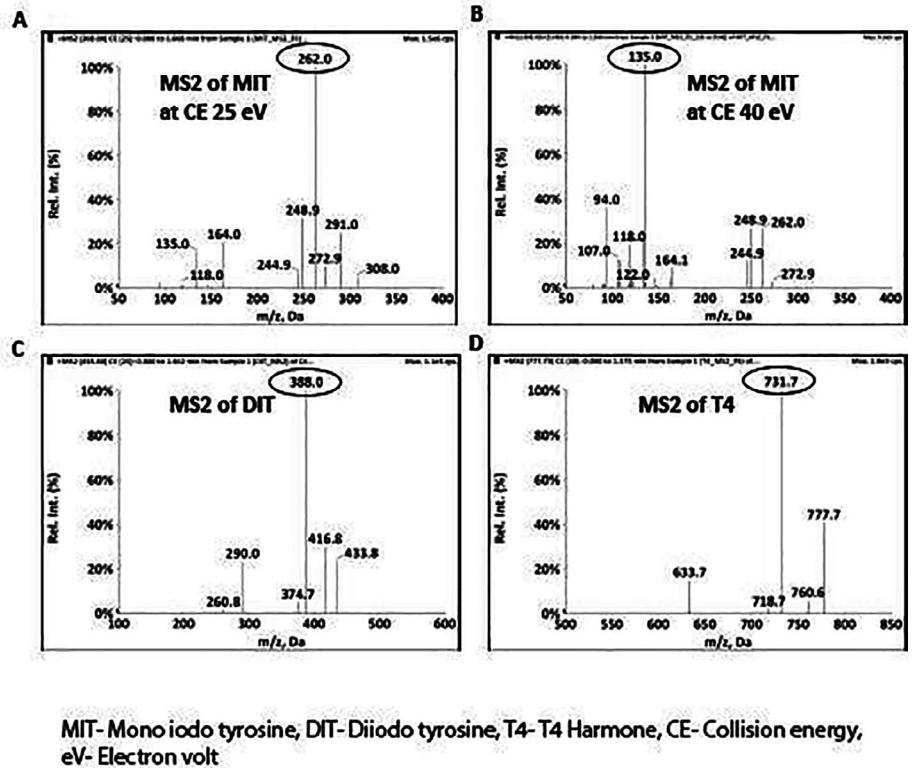

Fig. 1. Detection of MIT, DIT, and T4 by LC-MS/MS: A–D) MIT (A, B), DIT (C), and T4 (D) standards were infused at the concentration of 100 ng each, and their MS2 spectra were obtained as indicated. For MIT, two prominent fragment ions were considered for quantitative analysis at two different collision energies, 25 eV (A) and 40 eV (B). A single prominent fragment ion was considered for DIT (C) and T4 (D) analysis.

We have included rolipram as an internal standard during sample preparation to correct for variability due to analyte signal loss in sample pretreatment and storage. Results of the experiments could be expressed as the analyte peak area as well as the peak area ratio of the analyte to the internal standard.

3.2. TPO catalyzed generation of MIT from L-Tyr using rat thyroid microsomes

In vitro TPO activity assay was developed, which used isolated rat thyroid microsomes as the enzyme source. KI, H_2O_2, and L-Tyr were used as substrates for TPO. Conversion of L-Tyr to MIT was monitored by LC-MS/MS, as described in the Methods. Since at higher H_2O_2 concentrations, L-Tyr to MIT conversion could also occur in the absence of TPO, it was considered pertinent to optimize the effect of H_2O_2 on the iodination process. The assay was conducted in the presence (Fig. 2A), and absence (Supplementary Fig. 2C) of microsomes and time-dependent generation of MIT was monitored by LC-MS/MS.

In the presence of microsomes, the effect of H_2O_2 concentration was assessed within the range of 20 to 200 μM. A dose-dependent increase in MIT generation at 30 min and 60 min were observed as H_2O_2 concentration increased from 20 to 80 μM (Fig. 2A). At 10 min incubation time, dose dependence is not as obvious, and the least MIT levels were observed for 200 μM and highest for 40 μM. The overall pattern of time-dependent MIT generation at lower concentrations (20 μM − 80 μM) was different than at higher H_2O_2 (80 μM − 200 μM). Importantly, in the absence of microsomes background, MIT levels were negligible (Supplementary Fig. 2C). At the higher concentrations, there was a slight time-dependent increase in background MIT. However, it did not increase with time at 20 and 40 μM. Results were also expressed as peak area of analyte (Supplementary Fig. 2A).

In the absence of microsome, background MIT levels were negligible up to 80 μM H2O2 concentration. However, there was a subtle increase in MIT peak area ratio with time, at the higher H_2O_2 concentrations. At 40 μM H_2O_2, background MIT levels did not increase with time. Moreover, MIT generation in the presence of microsome at 10 min was highest at this concentration, indicating a high reaction rate. Thus, 40 μM H_2O_2 and the incubation period of 10 min was selected as an optimized concentration and use for all the L-Tyr to MIT assays hereafter.

It may be noted that there was a batch-to-batch variation in TPO activity. Hence, for each microsome batch, minimum background interference within the range of 20 to 200 μM H_2O_2 concentration was established by analyzing the generation of MIT from L-Tyr. Data

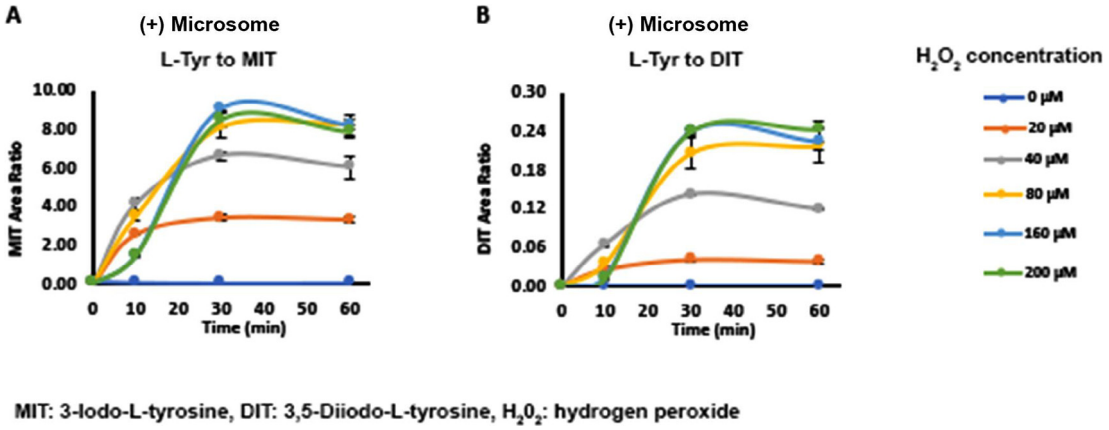

Fig. 2. Generation of MIT and DIT from L-Tyr in H_2O_2 dose-dependent manner: A, B) H_2O_2 dose-dependent generation of MIT (A) and DIT (B) from L-Tyr in the presence of rat thyroid microsomes was analyzed by LC-MS/MS. The time-dependent generation of analyte is represented as peak area ratios of analyte and rolipram (internal standard). The assay was conducted at 200, 160, 80, 40, 20, and 0 µM H_2O_2 concentration, using 10 µg microsomal protein, in a final volume of 250 µL, with 500 µM L-Tyr and 150 µM KI. One-way ANOVA Dunnett's multiple comparisons test for 30 min timepoint showed the p-value < 0.0001 (****) at all concentrations, when compared with control, Fig. 2(A). For Fig. 2(B) the p-value < 0.0001 (****) at concentrations 40–200 µM, and at 20 µM concentration the p-value were found to be 0.0272 (*).

from a different microsome batch (Batch II), isolated after a month gap, is shown in Supplementary Fig. 3. In the presence and the absence of microsomes, the ratio of MIT peak areas was expressed as MIT fold response. MIT fold response from the first batch (Batch I, Fig. 2A) and second batch (Batch II, Supplementary Fig. 3C) are compared. The batches with MIT fold response ≥ 50 and ≥ 15, at 30 min and 60 min, respectively, were considered acceptable for further use.

3.3. L-Tyr dose-dependent generation of DIT catalyzed by TPO

After successfully detecting the monoiodination of L-Tyr to MIT, the diiodination of L-Tyr was monitored by analyzing DIT levels by LC-MS/MS. Previous, studies using similar conditions detected MIT successfully but failed to detect DIT generated from L-Tyr using rat thyroid microsomes (Price et al., 2020). We aimed to optimize reaction conditions that favor the DIT generation. Moreover, as stated above, to know the influence of the H_2O_2 dose, the assay was performed at different concentrations of H_2O_2. Like MIT, DIT levels, measured in terms of analyte peak areas, increased as H_2O_2 concentration increased from 20 to 80 µM, at 30 and 60 min in the presence of microsomes. At 10 min, the least DIT levels were observed for 200 µM and highest for 40 µM (Fig. 2B), supporting a faster reaction rate.

Background DIT levels were nil for all the H_2O_2 concentrations in the absence of microsome, indicating high specificity and TPO dependence of conversion of L-Tyr to DIT (Supplementary Fig. 2D). DIT levels were also expressed as an analyte peak area (Supplementary Fig. 2B). Following the MIT pattern, initial DIT generation at 10 min was highest at 40 µM H_2O_2 concentration, moreover robust levels of both, MIT and DIT, were detected at 40 µM at all-time points, therefore the concentration of 40 µM H_2O_2 was kept constant in all the future L-Tyr to DIT assays.

Although specific, levels of DIT formed, were several folds lower than those of MIT, such low levels below the detection limit may be one reason for the failure of earlier researchers to detect it under similar experimental conditions by other investigators. One to one conversion of MIT to DIT may not be possible, but several-fold higher MIT levels suggested inefficient conversion of MIT to DIT. It is likely that, as the reaction progresses, L-Tyr and MIT, both being TPO substrates, could compete for the active sites, affecting the rate of reaction and the extent of product formation. Particularly, high concentrations of L-Tyr, 500 µM, might impair the generation of DIT from MIT. Therefore, to investigate the L-Tyr dose-dependent generation of DIT, the TPO assay was performed at different L-Tyr concentrations, keeping other conditions the same.

Both the L-Tyrosine disodium salt (Fig. 3, Supplementary Fig. 5) and non-salt L-Tyrosine (Supplementary Fig. 4) were evaluated for the formation of MIT and DIT during optimization of substrate concentrations. We found, MIT levels increased as tyrosine concentration increased from 100 µM to 1000 µM, as expected (Supplementary Fig. 4A, 5A). Contrary to MIT, DIT levels decreased as tyrosine concentration increased from 100 µM to 1000 µM (Supplementary Fig. 4B, 5B). Further, the impact of lower concentrations of L-Tyr, in the range of 0.5 mM – 100 µM, on MIT and DIT generation was also evaluated. At low L-Tyr concentrations, both MIT (Fig. 3A), as well as DIT (Fig. 3B), showed a dose-dependent increase in their levels from 0.5 µM to 50 µM. In line with the above results, DIT levels generated at 100 µM L-Tyr were lower than 25 µM L-Tyr.

Percent MIT and DIT generated with respect to the total product (MIT + DIT) generated in the reaction, at different time points were calculated to understand further the effect of tyrosine dose on the metabolism of these metabolites. DIT percentage increased from ~ 0.3% to ~ 3% to ~ 18%, as L-Tyrosine disodium salt concentration decreased from 1000 µM to 100 µM to 0.5 µM (Supplementary Fig. 5 D, F), respectively, accordingly, % MIT levels decreased, from ~ 99.6% to ~ 97% to ~ 82%, respectively (Supplementary Fig. 5 C, E).

The tyrosine concentration was kept in the range of 50–100 µM to obtain the robust response of MIT and DIT simultaneously, for subsequent experiments. Additionally, due to its better aqueous solubility, better dose-response, and ease of preparation, the disodium salt of L-Tyr was preferred for all future experiments.

3.4. Optimization of other assay parameters: KI concentration, pH, and microsomal protein content

Dose dependence of another TPO substrate, KI, on MIT and DIT formation was addressed by keeping other assay parameters constant. KI concentrations in the range of 25 µM to 300 µM were used at two fixed L-Tyr concentrations, 50 µM (Supplementary Fig. 7 A, B) and 100 µM (Supplementary Fig. 7C, D). MIT (Supplementary Fig. 7 A, C), as well as DIT (Supplementary Fig. 7B, D) formation, increased with increasing KI dose for both types of tyrosine at 50 as well as 100 µM concentration. Since the highest generation of MIT and DIT was observed at 300 µM, subsequent experiments were performed at this concentration. We believe this excess of the molar

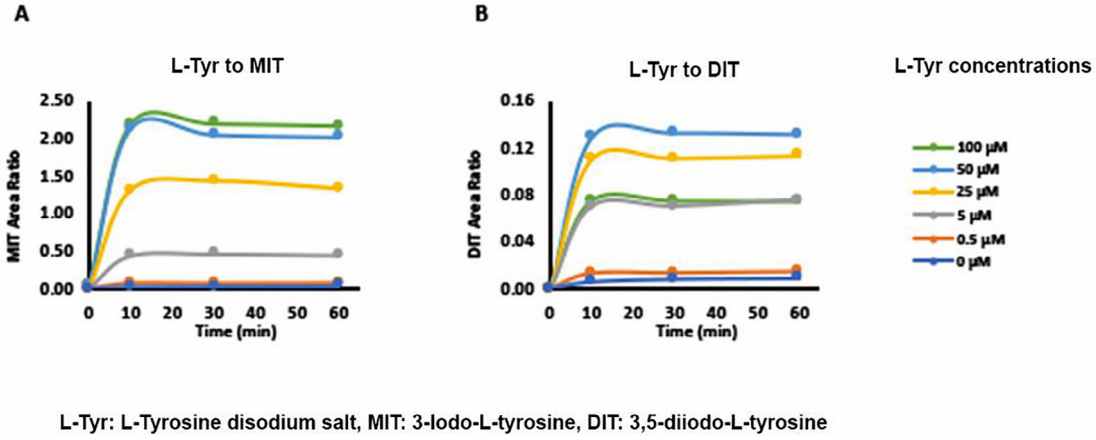

Fig. 3. Evaluation of MIT and DIT formation depending upon L-Tyr concentration: A, B) MIT (A) and DIT (B) formation were monitored by LC-MS/MS with varying concentrations of L- Tyr from 0.5 µM to 100 µM using 40 µM H_2O_2 and 150 µM KI.

equivalent of L-Tyr concentration of this reactant, KI, helps drive the reaction forward.

The effect of increasing levels of microsome protein concentrations on the generation of MIT and DIT was also examined to know the optimum microsomal protein content to be used in TPO assay. The protein amount mentioned is for a final volume of 250 µL or per assay (Supplementary Fig. 8). 5–10 µg protein appeared to be better suited for studying both metabolites, MIT and DIT, hence, most assays were conducted using this amount. We compared the efficacy of oxalic acid, formic acid, and sodium thiosulfate to quench TPO catalyzed reactions and confirmed that all of them are equally effective (Supplementary Fig. 9). However, as analyte signals were found to be highest with oxalic acid, it was used to stop the reaction.

3.5. Conversion of MIT to DIT, DIT to T4, and T3 to T4 monitored by LC-MS/MS

Having standardized the conditions for L-Tyr conversion to MIT, DIT, and their subsequent detection, the efforts were next to optimize the parameters to monitor the generation of THs within the same reaction. We could monitor the formation of MIT and DIT from L-Tyr. However, the formation of T3 and T4 from L-Tyr was not detected. This could be due to inefficient conversion of L-Tyr to T3 and T4, such that levels are below the detection limit. Alternatively, a necessary coupling of two tyrosine rings to synthesize T3 and T4 could need more optimization. To further elucidate TPO dependent catalysis, MIT, DIT and T3 were used as substrates and their conversion to subsequent metabolites was monitored by LC-MS/MS (Fig. 4, Supplementary Fig. 6). Representative data from two independent experiments at 0–200 µM (Supplementary Fig. 6A–C) and 200–600 µM (Fig. 4A-C) substrate concentration was shown. TPO substrates MIT (Fig. 4A, Supplementary Fig. 6A), DIT (Fig. 4B, Supplementary Fig. 6B), and T3 (Fig. 4C, Supplementary Fig. 6C) showed effective conversion into next reaction products.

MIT (Fig. 4A, Supplementary Fig. 6A) and T3 (Fig. 4C, Supplementary Fig. 6C) were converted to DIT and T4, respectively, indicating effective monoiodination of these compounds. DIT was converted to T4, indicating the successful coupling of two tyrosine rings (Fig. 4B, Supplementary Fig. 6B). Monoiodination of MIT and T3 could be observed at 10 min incubation for 5 and 25 µM. In contrast, tyrosine ring coupling of DIT to T4 was more efficient at concentration of a 600 µM at 10 min incubation. Technically, DIT to T4 conversion should not be dependent on iodination, as indicated by reasonable levels of T4 generated from 600 µM DIT in the absence of KI (-KI). However, the presence of KI significantly increased the conversion of 600 µM DIT to T4. Although MIT to DIT conversion was efficient at 5–25 µM, coupling of DIT to T4 could be detected only at concentrations above 200 µM.

To further characterize enzyme kinetics parameters for distinct TPO catalytic activities, data from each of the above-studied reactions were used to generate Michaelis-Menten curves using GraphPad Prism software (Supplementary Fig. 10A-D). Additionally, data from L-Tyr to MIT conversion was also processed to get Michaelis-Menten curves (Supplementary Fig. 10A). Obtained Km and Vmax values were further used to calculate the turnover number (K_{cat}) and catalytic efficiency (K_{cat}/K_m) (Supplementary Fig. 10E). As interpreted from the Km values, MIT affinity to TPO was highest, followed by L-Tyr, however, T3 and DIT affinities to TPO were weaker. Vmax values indicated that reaction rate was highest for L-Tyr to MIT conversion, followed by MIT to DIT and T3 to T4 reactions, whereas DIT to T4 conversion was slowest. Accordingly, the turnover rate of L-Tyr to MIT was highest, followed by MIT to DIT and T3 to T4. The lowest substrate affinity and least reaction rate resulted in minimum turnover (K_{cat}) in DIT to T4 reaction. Catalytic efficiency (K_{cat}/K_m) was highest for MIT to DIT conversion, followed by the conversion of L-Tyr to MIT. T3 to T4 catalytic efficiency was moderate, whereas DIT to T4 catalytic efficiency was very low.

3.6. Potency analysis of known inhibitors for TPO catalyzed individual reactions

With an elegant *in vitro* system to carry out a comprehensive analysis of distinct TPO enzymatic activities, known TPO inhibitors, ETU, PTU, Genistein (GST), Apigenin (AGN), Daidzein (DZN) were used to delineate their effects on individual catalytic activities mediated of TPO. L-Tyr, MIT, DIT, and T3 were used as substrates in the presence of an increasing concentration of these inhibitors, with testosterone as a negative control. Conversion of L-Tyr to MIT, L-Tyr to DIT, MIT to DIT, DIT to T4, and T3 to T4 was monitored by LC-MS/MS. Half maximal inhibitory concentration, IC50, a characteristic, quantitative measure of inhibitor potency of test chemical, was calculated using GraphPad Prism software for $N >= 3$ and standard deviation (SD) was reported as a measure of variability for the IC50 values (Fig. 5B). Four parametric sigmoidal IC_{50} curves of used chemicals for respective TPO reactions are shown with average IC_{50} values (Fig. 5A). Note that rat thyroid microsomes used in these experiments were from two different batches.

ETU, PTU, GST, and AGN inhibited MIT, MIT to DIT, and T3 to T4 reactions. The IC50 values were found to be between 0.807 µM and 4.854 µM for these substrates ($N \geq 3$). Whereas DZN, which has been

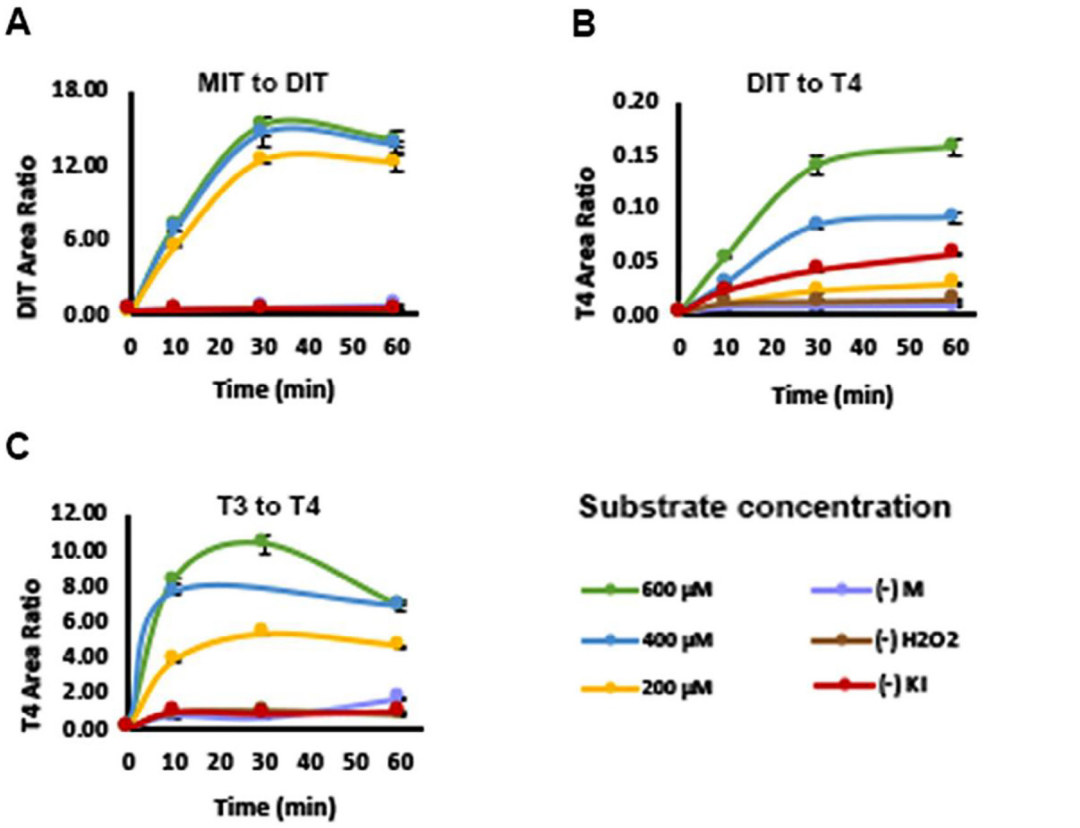

Fig. 4. Monitoring conversion of MIT to DIT, DIT to T4 and T3 to T4 by TPO: Substrate concentrations (600, 400 and 200 µM) of MIT (A), DIT (B), and T3 (C) were used for TPO activity analysis. Other assay conditions were constant as above. Conversion of MIT to DIT, DIT to T4, and T3 to T4 were monitored using LC-MS/MS. One-way ANOVA Dunnett's multiple comparison test for 30 min time point, showed the p-value < 0.0001 (****) at all concentrations of MIT, DIT and T3 when compared with respective control.

shown as a less potent inhibitor of TPO, showed higher IC_{50} values in the range of 19.74 µM to 57.31 µM. DZN also showed high variation in successive experiments, as reflected by the higher standard deviation. Overall, IC_{50} values of DIT to T4 conversion for ETU, PTU, GST, and AGN were relatively higher than IC_{50} values for their other reactions. These results suggest differential targeting of individual TPO catalyzed reactions by these inhibitors. Moreover, the inhibition profile of DZN is highly interesting and can be explored further to gain more insights into the TPO function as well as its targeting by xenobiotics.

4. Discussion

The goal of the study was to develop a battery of selective, sensitive, simple, and rapid *in vitro* assays to selectively discriminate between distinct catalytic activities of TPO. Such a battery of assays would provide more understanding about an organification of iodine into different substrates of TPO. These efforts led to the development of an assay method that helps quantitation of TH synthesis at five critical steps. A battery of simple *in vitro* assays that monitor the following five reactions was developed successfully, L-Tyr to MIT, L-Tyr to DIT, MIT to DIT, T3 to T4, and DIT to T4.

Previously reported *in vitro* TPO activity assays studied iodination of purified and recombinant thyroglobulin in the presence of iodide and H_2O_2 (Celi et al., 2008). Alternatively, many studies have also examined iodination of the pseudo substrates, such as albumin, or physiologically more relevant, tyrosine containing peptides as well as free tyrosine. Partially purified TPO or isolated microsomes from the thyroid of human, rat, pig and other species, are the routine source of enzyme used in these assays.

Assays that detect the generation of THs and their intermediates in thyroglobulin are limited by longer time reactions, cumbersome isolation, and analysis of thyroglobulin as well as their low sensitivities. Some of the published methods, also involve the use of radioactive iodine for the TPO assay (Turner & Tipton, 1971; Vannucchi et al., 2009). HPLC or LC-MS based assays that study L-Tyr conversion into MIT and DIT fill this gap and have been described before (Divi & Doerge, 1996; Freyberger & Ahr, 2006; Kasai et al., 1989; Price et al., 2020). Compared to HPLC, LC-MS/MS detection is much more sensitive and rapid. Such an assay to monitor the conversion of L-Tyr to MIT by LC-MS/MS was reported recently (Price et al., 2020).

LC-MS/MS-based detection method of the above reaction products was highly selective, sensitive, simple, and rapid. We explored MRM, a powerful analytical tool that monitors highly selective mass transitions of a compound in complex mixtures (Zhang et al., 2016). The selected predominant daughter ions with *m/z*, 262 and 135 for MIT, 388 for DIT, and 732 for T4 matched with the previous studies, supporting high specificity (Hornung et al., 2015; Yang et al., 2016). We con-

A

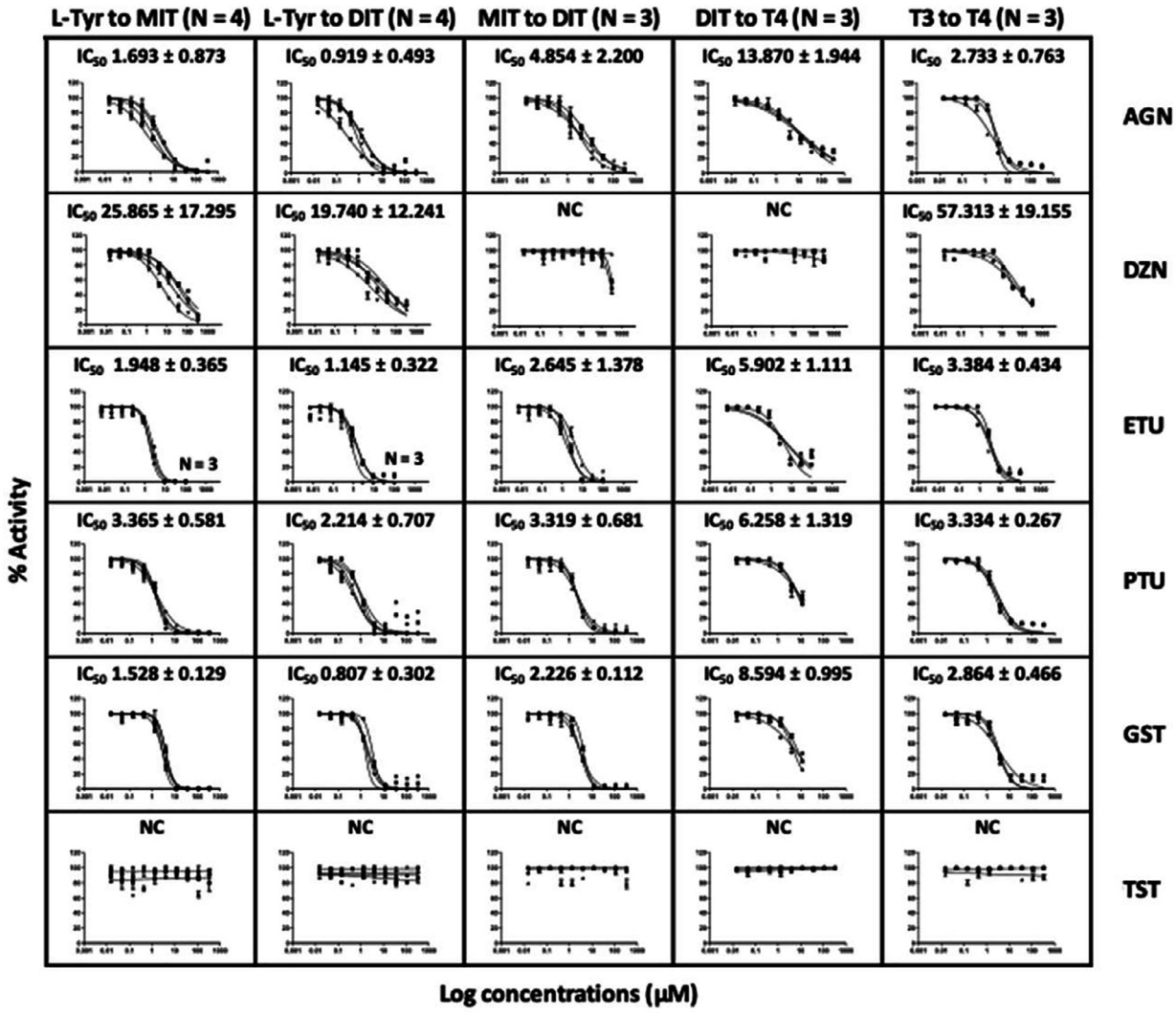

B

Test Chemicals	L-Tyr to MIT (N=4)		L-Tyr to DIT (N=4)		MIT to DIT (N=3)		DIT to T4 (N=3)		T3 to T4 (N=3)	
	IC50	SD	IC50	SD	IC50	SD	IC50	SD	IC50	SD
AGN	1.693	0.873	0.919	0.493	4.854	2.200	13.870	1.944	2.733	0.763
DZN	25.865 *	17.295	19.740 *	12.241	NC	-	NC	-	57.313	19.155
ETU	1.948 *	0.365	1.145 *	0.322	2.645	1.378	5.902	1.111	3.384	0.434
PTU	3.365	0.581	2.214	0.707	3.319	0.681	6.258	1.319	3.334	0.267
GST	1.528	0.129	0.807	0.302	2.226	0.112	8.594	0.995	2.864	0.466
TST	NC	-	NC	-	NC	-	NC	-	NC	-

*N=3

L-Tyr: L-Tyrosine disodium salt, MIT: 3-Iodo-L-tyrosine, DIT: 3,5 Diiodo-L-tyrosine, T3: 3,3',5- Triiodo-L-thyronine, T4: Levothyroxine, AGN: Apigenin, DZN: Daidzein, ETU: Ethylenethiourea, PTU: 6-Propyl -2-thiouracil, GST: Genistein, TST: Testosterone, IC50: Half maximum inhibitory concentration, NC: Not converged

Fig. 5. Inhibition of multiple TPO catalyzed reactions by AGN, DDZ, ETU, GST, and PTU: A) Graphs illustrating log of inhibitor concentration v/s % activity was plotted as per four parametric fits using GraphPad Prism. The individual reaction catalyzed by TPO, with the corresponding substrate is indicated. TST was taken as a negative control. IC50 values (inhibitor concentration which produces 50% enzyme inhibition) for each reaction with respective inhibitors are shown. B) Table illustrating IC50 ± SDs for multiple TPO catalyzed reactions with respective inhibitors are shown. Values obtained using four-parameter equation from GraphPad Prism ($N \geq 3$). * indicates $N = 3$. NC indicates Not converged, showing that IC50 value cannot be determined.

firmed the linear response in the range of a few picomolar to several hundreds of nanomolar for all three analytes (Supplementary Fig. 1). Moreover, there was no effect of matrix on ionization or detection of analytes of interests within the above concentration range, suggesting high sensitivity. We established a single, robust method using LC-MS/MS for all the analytes used throughout the study. Moreover, we confirmed that the extraction efficiency for MIT, DIT, and T4 analytes was highly consistent.

Preliminary efforts aimed at minimizing the background interference by ensuring high TPO activity in isolated microsome was optimizing H_2O_2 concentration. Microsome batches with high TPO activity were validated with simple criteria of acceptable MIT fold response. An example of a rejected microsome batch is shown to accentuate the importance of high TPO activity for specific monitoring of TPO catalyzed reaction (Supplementary Fig. 11). Usage of optimized H_2O_2 concentration ensured that background correction was not required in the setup.

The previously published assays detected the change in indicator dye color, fluorescence, or luminescence, which was possibly driven by the change in Oxidation-Reduction potential (O/R) of the test system.

The method described here provides comprehensive information about distinct steps in TH synthesis catalyzed by TPO. The use of L-Tyr, MIT, DIT, and T3 as TPO substrates is physiologically more relevant, than any pseudosubstrate. Unlike the above assays, which must be read for the signal within a specific time, there is no loss of signal with time. Even after 48 h, samples can be analyzed efficaciously, with our method. Like the guaiacol method, continuous reaction monitoring is not possible with the assays described here (Paul et al., 2014). However, enzyme kinetic analysis was efficiently performed with our method.

Two-electron transfer iodination of L-Tyr and MIT, catalyzed by TPO, are chemically identical, electrophilic substitution reactions (Nakamura et al., 1984). Comparison of iodination of L-Tyr to MIT and DIT (Fig. 3, Supplementary Fig. 5), MIT to DIT (Fig. 4A, Supplementary Fig. 6A), and T3 to T4 (Fig. 4C, Supplementary Fig. 6C) at fixed, 40 μM H_2O_2 showed subtle differences.

Direct and linear correlation between substrate dose and product formation was observed over a wide range of substrate concentrations. However, the enzyme kinetic analysis showed that these three reactions proceeded differently. This was further investigated for affinity to TPO and the rates of reaction with the four substrates. It was observed that the affinity of different substrates to TPO followed the following pattern: MIT to DIT > L-Tyr to MIT > T3 to T4 > DIT to T4. On the other hand, the Vmax relations appeared to indicate; L-Tyr to MIT > MIT to DIT > T3 to T4 > DIT to T4. These data support substrate-dependent differences in three monoiodination reactions and one coupling reaction between two molecules of DIT to T4.

On the other hand, the diiodination of L-Tyr to DIT is a two-step reaction; L-Tyr to MIT and MIT to DIT (Nakamura et al., 1984). Such two-step reactions constrain adaptability for the Michaelis-Menten curve generation for L-Tyr to DIT. This could be due to the different reaction rates between L-Tyr to MIT, followed by iodination of MIT to DIT. DIT generation showed an inverse correlation with substrate concentration in the range of 100–1000 μM substrate. Thus, L-Tyr concentration appears to be a regulatory switch between mono- and diiodination reactions mediated by TPO. High L-Tyr levels favor monoiodination, while the lower range, favors diiodination.

Previous studies reported that the peroxidase is much more efficient at the coupling of two DIT molecules than MIT and DIT. This is supported by a predominant synthesis of T4 over T3 in the thyroid gland (Citterio et al., 2019). Accordingly, results presented here show that the *in vitro* generation of T4 from DIT could be monitored successfully. However, the development of an assay to show coupling between MIT and DIT to generate T3 was unsuccessful. Compared to the monoiodination reactions, much smaller peak area ratios were observed indicating an inefficient intramolecular coupling of iodotyrosyl residues by TPO. The DIT to T4 reaction appears to occur only at high DIT concentrations (Fig. 4B, Supplementary Fig. 6B). Overall, the data validates several earlier reports that iodination and coupling are two distinct types of reactions catalyzed by TPO (Taurog et al., 1996). Additionally, the results also reveal the discrete specificity of TPO towards different substrates. Distinct K_m, Vmax, K_{cat} and K_{cat}/K_m values suggest that each of these reactions can be studied independently.

Reports about the specificity of iodination reactions available in the literature are confounding (Carvalho & Dupuy, 2017; Kessler et al., 2008). Few studies suggest that the nonspecific reactions are favored when reactive iodine species are released from TPO which iodinate tyrosines randomly. In contrast to this specific reaction would take place when TPO binding of both substrates (i.e., iodine and L-Tyr/MIT/DIT), facilitates iodination. Our studies suggest of a specific iodination of the individual substrates of TPO. Although iodination and coupling of free substrates such as L-Tyr, MIT, DIT, T3 and thyroglobulin residues, cannot be compared, it is interesting to note that out of 66 available tyrosine residues in thyroglobulin only 25–30 are iodinated, of which 5–16 are coupled to form 2–16 molecules of TH (Citterio et al., 2019; Coscia et al., 2020). This observation supports the existence of high specificity by which tyrosines undergo TH synthesis. Structural determinants of thyroglobulin and exposure of iodine residues appear to be another key factor (Coscia et al., 2020).

As described in Fig. 2, 3, 5 and Supplementary Figs. 2–5, 7–11; the generation of MIT and DIT from L-Tyr in one reaction, make it possible to analyze monoidination, and diiodination reactions in a single assay. Developing similar assays that allow investigation of multiple sequential reactions such as iodination and coupling may be challenging, but it can be achieved by optimizing the assay conditions. Increased DIT generation at low L-Tyr levels, supports this assumption. Decreased competition from L-Tyr concentration, most likely promotes the conversion of MIT to DIT. However, the role of other metabolic regulatory mechanisms cannot be ruled out. By acting as a shuttle for the transfer of oxidizing equivalents, free DIT was shown to regulate the coupling of iodotyrosine residues in thyroglobulin (Taurog et al., 1996). Importantly, it is worth noting that free MIT, DIT along with T3 and T4 are readily made available in thyroids upon proteolysis of thyroglobulin (Baudry et al., 1997). It will be valuable to explore further the regulation of TPO activity and TH synthesis by studying individual reactions, amongst these metabolites.

IC_{50} analysis of known TPO inhibitors GST, AGN, ETU, PTU, and DZN were carried out to assess their inhibition potential toward individual TPO reactions. Unlike, GST, AGN, ETU, and PTU, literature data for DZN potency is inconsistent. Reported IC_{50} values vary from 1.8 μM to 33 μM (Divi et al., 1997; Paul et al., 2014). We also experienced high experimental variation in DZN IC_{50} values. DZN inhibited L-Tyr to MIT and DIT, as well as T3 to T4 iodination. Intriguingly, it had no adverse effects on MIT to DIT iodination. There is a high resemblance between the chemical structures of three, GST, and DZN are trihydroxy and dihydroxy isoflavones, respectively, whereas AGN belongs to the trihydroxy flavone group (Chang & Doerge, 2000; Divi et al., 1997; Doerge & Chang, 2002). Differential inhibition of TPO activities by DZN further supports the independent nature of multiple reactions catalyzed by TPO. The observations of the assay described herein, underscore the effectiveness of the assay to distinguish between the modes of action of the inhibitors of TPO.

Multifaceted enzymes like TPO can be inhibited at multiple different steps. Engler *et al.* established that PTU and methylmercaptoimidazole (MMI) could exert a specific inhibitory effect on the coupling reaction. In the case of PTU, a specific inhibitory effect on coupling was also demonstrated with an incubation system in which TPO-catalyzed coupling was measured in the absence of iodination. T4 formation was considerably more sensitive to the inhibitory actions of PTU and MMI than was total iodination or formation of DIT (Engler

et al., 1982). Moreover, antioxidants, heme interacting chemicals, or entities that interfere with electrophilic substitution can also affect TPO activity in *in vitro* assays. While investigating these multiple ways by which xenobiotics can impair TPO activity *in vitro*, it is also important to validate obtained data using in vivo systems and correlate the findings from TPO inhibition studies with thyroid-specific adverse outcomes. Therefore, we propose more measured, and nuanced strategies that can provide mechanistic understandings of the TPO function as described here.

5. Conclusion

We propose a novel *in vitro* strategy to evaluate the multifaceted catalytic functions of TPO. The proposed approach involves an analysis of mono- and di-iodination activities as well as investigation of coupling of iodinated tyrosyl rings catalyzed by TPO, using a battery of independent assays. Results substantiate the distinct catalytic activities of TPO with unique enzyme kinetic parameters. Conversion of L-Tyr to MIT, L-Tyr to DIT, MIT to DIT, T3 to T4, and DIT to T4 in the presence of thyroid microsomes can now be studied by highly selective, sensitive, simple, and rapid LC-MS/MS based method. Importantly, studies with known inhibitors revealed their differential impact on discrete TPO activities. Thus, with this novel approach it is possible to delineate, and distinguish between, the mode of action of varied TPO inhibitors. Overall, the above approach will enable much better, and thorough understanding of the catalytic function of TPO. Additionally, future characterization of compounds depending upon their respective action on distinct TPO activities will facilitate pertinent labeling and categorization of diverse TPO inhibitors.

Declaration of Competing Interest

The authors declare that they have no known competing financial interests or personal relationships that could have appeared to influence the work reported in this paper.

Appendix A. Supplementary data

Supplementary data to this article can be found online at https://doi.org/10.1016/j.crtox.2021.01.001.

References

Abas, L., Luschnig, C., 2010. Maximum yields of microsomal-type membranes from small amounts of plant material without requiring ultracentrifugation. Anal. Biochem. 401 (2), 217–227. https://doi.org/10.1016/j.ab.2010.02.030.

Baudry, N., Mallet, B., Lejeune, P.J., Vinet, L., Franc, J.L., 1997. A micromethod for quantitative determination of iodoamino acids in thyroglobulin. J. Endocrinol.. https://doi.org/10.1677/joe.0.1530099.

Bianco, A.C., Kim, B.W., 2006. Deiodinases: implications of the local control of thyroid hormone action. J. Clin. Investig. 116 (10), 2571–2579. https://doi.org/10.1172/JCI29812.

Boas, M., Feldt-Rasmussen, U., Main, K.M., 2012. Thyroid effects of endocrine disrupting chemicals. Mol. Cell. Endocrinol. 355 (2), 240–248. https://doi.org/10.1016/j.mce:2011.09.005.

Carvalho, D.P., Dupuy, C., 2017. Thyroid hormone biosynthesis and release. Mol. Cell. Endocrinol. 458, 6–15. https://doi.org/10.1016/j.mce:2017.01.038.

Celi, F. S., Coppotelli, G., Chidakel, A., Kelly, M., Brillante, B. A., Shawker, T., Cherman, N., Feuillan, P. P., & Collins, M. T. (2008). The role of type 1 and type 2 5′-deiodinase in the pathophysiology of the 3,5,3′-triiodothyronine toxicosis of McCune-Albright syndrome. Journal of Clinical Endocrinology and Metabolism. https://doi.org/10.1210/jc.2007-2237.

Chang, H.C., Doerge, D.R., 2000. Dietary genistein inactivates rat thyroid peroxidase in vivo without an apparent hypothyroid effect. Toxicol. Appl. Pharmacol. 168 (3), 244–252. https://doi.org/10.1006/taap.2000.9019.

Chung, J.K., 2002. Sodium iodide symporter: its role in nuclear medicine. J. Nucl. Med..

Citterio, C.E., Targovnik, H.M., Arvan, P., 2019. The role of thyroglobulin in thyroid hormonogenesis. Nat. Rev. Endocrinol. 15 (6), 323–338. https://doi.org/10.1038/s41574-019-0184-8.

Coady, K., Marino, T., Thomas, J., Currie, R., Hancock, G., Crofoot, J., McNalley, L., McFadden, L., Geter, D., Klecka, G., 2010. Evaluation of the amphibian metamorphosis assay: exposure to the goitrogen methimazole and the endogenous thyroid hormone L-thyroxine. Environ. Toxicol. Chem. 29 (4), 869–880. https://doi.org/10.1002/etc.74.

Coscia, F., Taler-Verčič, A., Chang, V.T., Sinn, L., O'Reilly, F.J., Izoré, T., Renko, M., Berger, I., Rappsilber, J., Turk, D., Löwe, J., 2020. The structure of human thyroglobulin. Nature 578 (7796), 627–630. https://doi.org/10.1038/s41586-020-1995-4.

Davidson, B., Neary, J.T., Strout, H.V., Maloof, F., Soodak, M., 1978a. Evidence for a thyroid peroxidase associated "active iodine" species. Biochim. Biophys. Acta (BBA) – Enzymol. 522 (2), 318–326. https://doi.org/10.1016/0005-2744(78)90066-9.

Davidson, Betty, Soodak, Morris, Neary, Joseph T., Vincent Strout, H., David Kieffer, J., Mover, Heidi, Maloof, Farahe, 1978b. The irreversible inactivation of thyroid peroxidase by methylmercaptoimidazole, thiouracil, and propylthiouracil in vitro and its relationship to in vivo findings*. Endocrinology 103 (3), 871–882. https://doi.org/10.1210/endo-103-3-871.

Divi, R.L., Chang, H.C., Doerge, D.R., 1997. Anti-thyroid isoflavones from soybean. Biochem. Pharmacol. 54 (10), 1087–1096. https://doi.org/10.1016/S0006-2952(97)00301-8.

Divi, R.L., Doerge, D.R., 1996. Inhibition of thyroid peroxidase by dietary flavonoids. Chem. Res. Toxicol. 9 (1), 16–23. https://doi.org/10.1021/tx950076m.

Doerge, D.R., Chang, H.C., 2002. Inactivation of thyroid peroxidase by soy isoflavones, in vitro and in vivo. J. Chromatogr. B 777 (1-2), 269–279. https://doi.org/10.1016/S1570-0232(02)00214-3.

Engler, Hanna, Taurog, Alvin, DORRIS, Martha L., 1982. Preferential inhibition of thyroxine and 3,5,3′-triiodothyronine formation by propylthiouracil and methylmercaptoimidazole in thyroid peroxidase-catalyzed iodination of thyroglobulin*. Endocrinology 110 (1), 190–197. https://doi.org/10.1210/endo-110-1-190.

EPA - Series 890. (2009). https://www.epa.gov/test-guidelines-pesticides-and-toxic-substances/final-test-guidelines-pesticides-and-toxic.

Ferreira, A.C.F., Rosenthal, D., Carvalho, D.P., 2000. Thyroid peroxidase inhibition by Kalanchoe brasiliensis aqueous extract. Food Chem. Toxicol. 38 (5), 417–421. https://doi.org/10.1016/S0278-6915(00)00017-X.

Fini, J.-B., Mughal, B.B., Le Mével, S., Leemans, M., Lettmann, M., Spirhanzlova, P., Affaticati, P., Jenett, A., Demeneix, B.A., 2017. Human amniotic fluid contaminants alter thyroid hormone signalling and early brain development in Xenopus embryos. Sci. Rep. 7 (1). https://doi.org/10.1038/srep43786.

Freyberger, A., Ahr, H., 2006. Studies on the goitrogenic mechanism of action of N,N,N′, N′-tetramethylthiourea. Toxicology 217 (2-3), 169–175. https://doi.org/10.1016/j.tox.2005.09.005.

Paul Friedman, K., Watt, E.D., Hornung, M.W., Hedge, J.M., Judson, R.S., Crofton, K.M., Houck, K.A., Simmons, S.O., 2016. Tiered high-throughput screening approach to identify thyroperoxidase inhibitors within the ToxCast Phase I and II chemical libraries. Toxicol. Sci. 151 (1), 160–180. https://doi.org/10.1093/toxsci/kfw034.

Gilbert, M.E., Rovet, J., Chen, Z., Koibuchi, N., 2012. Developmental thyroid hormone disruption: Prevalence, environmental contaminants and neurodevelopmental consequences. NeuroToxicology 33 (4), 842–852. https://doi.org/10.1016/j.neuro.2011.11.005.

Guo, B., Chen, B., Liu, A., Zhu, W., Yao, S., 2012. Liquid chromatography-mass spectrometric multiple reaction monitoring-based strategies for expanding targeted profiling towards quantitative metabolomics. Curr. Drug Metab.. https://doi.org/10.2174/138920012803341401.

Haselman, J.T., Olker, J.H., Kosian, P.A., Korte, J.J., Swintek, J.A., Denny, J.S., Nichols, J.W., Tietge, J.E., Hornung, M.W., Degitz, S.J., 2020. Targeted pathway-based in vivo testing using thyroperoxidase inhibition to evaluate plasma thyroxine as a surrogate metric of metamorphic success in model amphibian xenopus laevis. Toxicol. Sci.. https://doi.org/10.1093/toxsci/kfaa036.

Hornung, M.W., Degitz, S.J., Korte, L.M., Olson, J.M., Kosian, P.A., Linnum, A.L., Tietge, J.E., 2010. Inhibition of thyroid hormone release from cultured amphibian thyroid glands by methimazole, 6-propylthiouracil, and perchlorate. Toxicol. Sci.. https://doi.org/10.1093/toxsci/kfq166.

Hornung, M.W., Kosian, P.A., Haselman, J.T., Korte, J.J., Challis, K., Macherla, C., Nevalainen, E., Degitz, S.J., 2015. In Vitro, Ex Vivo , and In Vivo Determination of Thyroid Hormone Modulating Activity of Benzothiazoles. Toxicol. Sci. 146 (2), 254–264. https://doi.org/10.1093/toxsci/kfv090.

Hosoya, T., Morrison, M., 1965. The peroxidase and other hemoproteins of thyroid microsomes. Biochem. Biophys. Res.. Communications.

Kaczur, V., Vereb, G., Molnar, I., Krajczar, G., Kiss, E., Farid, N. R., & Balazs, C. (1997). Effect of anti-thyroid peroxidase (TPO) antibodies on TPO activity measured by chemiluminescence assay. Clinical Chemistry. https://doi.org/10.1093/clinchem/43.8.1392

Kasai, K., Ohmori, T., Koizumi, N., Hosoya, T., Hiraiwa, M., Emoto, T., Hattori, Y., Shimoda, S.-I., 1989. Regulation of thyroid peroxidase activity by thyrotropin, epidermal growth factor and phorbol ester in porcine thyroid follicles cultured in suspension. Life Sci. 45 (16), 1451–1459. https://doi.org/10.1016/0024-3205(89)90035-0.

Kessler, J., Obinger, C., Eales, G., 2008. Factors Influencing the Study of Peroxidase-Generated Iodine Species and Implications for Thyroglobulin Synthesis. Thyroid 18 (7), 769–774. https://doi.org/10.1089/thy.2007.0310.

Kootstra, P. R., Wever, R., & De Vijlder, J. J. M. (1993). Thyroid peroxidase: Kinetics, pH optima and substrate dependency. Acta Endocrinologica. https://doi.org/10.1530/acta.0.1290328.

Lerro, C.C., Beane Freeman, L.E., DellaValle, C.T., Kibriya, M.G., Aschebrook-Kilfoy, B., Jasmine, F., Koutros, S., Parks, C.G., Sandler, D.P., Alavanja, M.C.R., Hofmann, J.N., Ward, M.H., 2018. Occupational pesticide exposure and subclinical hypothyroidism among male pesticide applicators. Occup. Environ. Med. 75 (2), 79–89. https://doi.org/10.1136/oemed-2017-104431.

Martin, M. T., Brennan, R. J., Hu, W., Ayanoglu, E., Lau, C., Ren, H., Wood, C. R., Corton, J. C., Kavlock, R. J., & Dix, D. J. (2007). Toxicogenomic study of triazole fungicides and perfluoroalkyl acids in rat livers predicts toxicity and categorizes chemicals based on mechanisms of toxicity. Toxicological Sciences. https://doi.org/10.1093/toxsci/kfm065

Martin, M.T., Judson, R.S., Reif, D.M., Kavlock, R.J., Dix, D.J., 2009. Profiling chemicals based on chronic toxicity results from the U.S. EPA ToxRef database. Environ. Health Perspect. 117 (3), 392–399. https://doi.org/10.1289/ehp.0800074.

Mclachlan, Sandra. M., Rapoport, Basil, 1992. The molecular biology of thyroid peroxidase: cloning, expression and role as autoantigen in autoimmune thyroid disease*. Endocr. Rev. 13 (2), 192–206. https://doi.org/10.1210/edrv-13-2-192.

Motonaga, K., Ota, M., Odawara, K., Saito, S., Welsch, F., 2016. A comparison of potency differences among thyroid peroxidase (TPO) inhibitors to induce developmental toxicity and other thyroid gland-linked toxicities in humans and rats. Regul. Toxicol. Pharm. 80, 283–290. https://doi.org/10.1016/j.yrtph.2016.06.019.

Nakamura, M., Yamazaki, I., Nakagawa, H., Ohtaki, S., Ui, N., 1984. Iodination and oxidation of thyroglobulin catalyzed by thyroid peroxidase.. J. Biol. Chem. 259 (1), 359–364. https://doi.org/10.1016/S0021-9258(17)43667-2.

Gd, O.E.C.D., 150., 2018. Revised Guidance Document 150 on Standardised Test Guidelines for Evaluating Chemicals for Endocrine Disruption. In *OECD Series on Testing and Assessment*.

Orloff, Lisa A., Wiseman, Sam M., Bernet, Victor J., Fahey III, Thomas J., Shaha, Ashok R., Shindo, Maisie L., Snyder, Samuel K., Stack Jr., Brendan C., Sunwoo, John B., Wang, Marilene B., 2018. American thyroid association statement on postoperative hypoparathyroidism: diagnosis, prevention, and management in adults. Thyroid 28 (7), 830–841. https://doi.org/10.1089/thy.2017.0309.

Paul, Katie B., Hedge, Joan M., Rotroff, Daniel M., Hornung, Michael W., Crofton, Kevin M., Simmons, Steven O., 2014. Development of a Thyroperoxidase Inhibition Assay for High-Throughput Screening. Chem. Res. Toxicol. 27 (3), 387–399. https://doi.org/10.1021/tx400310w.

Pirahanchi, Y., Toro, F., & Jialal, I. (2020). Physiology, Thyroid Stimulating Hormone. StatPearls.

Portman, Michael A., 2008. Thyroid hormone regulation of heart metabolism. Thyroid 18 (2), 217–225. https://doi.org/10.1089/thy.2007.0257.

Price, Roger J., Burch, Rachel, Chatham, Lynsey R., Higgins, Larry G., Currie, Richard A., Lake, Brian G., 2020. An assay for screening xenobiotics for inhibition of rat thyroid gland peroxidase activity. Xenobiotica 50 (3), 318–322. https://doi.org/10.1080/00498254.2019.1629044.

Serrano, Jose, Higgins, LeeAnn, Witthuhn, Bruce A., Anderson, Lorraine B., Markowski, Todd, Holcombe, Gary W., Kosian, Patricia A., Korte, Joseph J., Tietge, Joseph E., Degitz, 2010. In vivo assessment and potential diagnosis of xenobiotics that perturb the thyroid pathway: Proteomic analysis of Xenopus laevis brain tissue following exposure to model T4 inhibitors. Comp. Biochem. Physiol. D Genom. Proteom. 5 (2), 138–150. https://doi.org/10.1016/j.cbd.2010.03.007.

Taurog, Alvin, Dorris, Martha L., Doerge, Daniel R., 1996. Mechanism of simultaneous iodination and coupling catalyzed by thyroid peroxidase. Arch. Biochem. Biophys. 330 (1), 24–32. https://doi.org/10.1006/abbi.1996.0222.

Tazebay, Uygar H., Wapnir, Irene L., Levy, Orlie, Dohan, Orsolya, Zuckier, Lionel S., Hua Zhao, Qing, Fu Deng, Hou, Amenta, Peter S., Fineberg, Susan, Pestell, Richard G., Carrasco, Nancy, 2000. The mammary gland iodide transporter is expressed during lactation and in breast cancer. Nat. Med. 6 (8), 871–878. https://doi.org/10.1038/78630.

Tietge, Joseph E., Butterworth, Brian C., Haselman, Jonathan T., Holcombe, Gary W., Hornung, Michael W., Korte, Joseph J., Kosian, Patricia A., Wolfe, Marilyn, Degitz, Sigmund J., 2010. Early temporal effects of three thyroid hormone synthesis inhibitors in Xenopus laevis. Aquat. Toxicol. 98 (1), 44–50. https://doi.org/10.1016/j.aquatox.2010.01.014.

Tietge, Joseph E., Holcombe, Gary W., Flynn, Kevin M., Kosian, Patricia A., Korte, Joseph J., Anderson, Leroy E., Wolf, Douglas C., Degitz, Sigmund J., 2005. Metamorphic inhibition of Xenopus laevis by sodium perchlorate: effects on development and thyroid histology. Environ. Toxicol. Chem. 24 (4), 926–933. https://doi.org/10.1897/04-105R.1.

Turner, James E., Tipton, Samuel R., 1971. The role of the lizard thyroid gland in tail regeneration. J. Exp. Zool. 178 (1), 63–85. https://doi.org/10.1002/jez.1401780110.

Vannucchi, G., Campi, I., Covelli, D., Dazzi, D., Currò, N., Simonetta, S., Ratiglia, R., Beck-Peccoz, P., Salvi, M., 2009. Graves' orbitopathy activation after radioactive iodine therapy with and without steroid prophylaxis. J. Clin. Endocrinol. Metabol.. https://doi.org/10.1210/jc.2009-0506.

Yang, Yijun, Peng, Yue'e, Chang, Qing, Dan, Conghui, Guo, Wei, Wang, Yanxin, 2016. Selective identification of organic iodine compounds using liquid chromatography–high resolution mass spectrometry. Anal. Chem. 88 (2), 1275–1280. https://doi.org/10.1021/acs.analchem.5b03694.s001.

Younggren, N. A., & Hadley, M. E. (1981). Thyroid Hormones and Amphibian Metamorphosis. American Biology Teacher. https://doi.org/10.2307/4447109

Zhang, Yan Victoria, Wei, Bin, Zhu, Yu, Zhang, Yanhua, Bluth, Martin H., 2016. Liquid chromatography–tandem mass spectrometry. Clin. Lab. Med. 36 (4), 635–661. https://doi.org/10.1016/j.cll.2016.07.001.